# Solvation of KSCN in Water

**A. Botti, S. E. Pagnotta,† F. Bruni, and M. A. Ricci***

*Dipartimento di Fisica "E. Amaldi", Università degli Studi "Roma Tre", Via della Vasca Navale 84, 00146 Roma, Italy*

*Received: April 15, 2009; Revised Manuscript Received: May 28, 2009*

The results of a neutron diffraction experiment performed on aqueous solutions of KSCN are analyzed and discussed in comparison with similar data for KCl and KOH solutions. The effect of the different ions on the structure of water and the differences and similarities among the ion solvation shells are discussed in detail. In particular it is shown that the effect of KSCN on the structure of water is visible as a shift and a broadening of the second peak of the oxygen−oxygen radial distribution function, which corresponds to a lower number of interstitial water molecules, compared to pure water. The hydration shell of the cation is similar to that found in the case of KCl solutions, and more interestingly the hydration shell of $SCN^-$ is asymmetric, with water molecules H-bonded to the N site and weakly correlated to the S site. These results provide a reasonable microscopic description of the mechanism for the high efficiency of thiocyanate in crystallizing basic proteins.

## I. Introduction

Over the past few years we have intensively investigated the microscopic structure of aqueous solutions of monovalent ions[1−9] in a wide range of concentration and ionic size. These studies have shown that the effect of ions on the microscopic structure of water is not limited to the first ion hydration shell,[7] contrarily to what is observed by experiments, which probe the single molecule relaxation dynamics.[10,11] The disturbance of the water−water spatial correlations in the presence of monovalent ions does indeed extend throughout the hydrogen-bond network and is manifested as a shift of the second peak of the oxygen−oxygen radial distribution function, $g_{OwOw}(r)$, to shorter distances compared to pure water. This is visible also when the molecules in the ion hydration shell are not included in the calculation of the radial distribution function (RDF).[7] Such effect on the $g_{OwOw}(r)$ function can be assimilated to that of an external pressure on pure water.[4,12] Moreover previous work has brought to light the weakness and contradictions of the classical concepts of an ion being "structure maker" or "breaker".[8] By comparing the experimental results obtained in the case of salt or hydroxide solutions, we have indeed shown that, if we look at the cation hydration shell, the orientational distribution of water molecules may be broader around one ion compared to another, so that one could infer the first ion being "structure breaker" as opposed to the second being "structure maker". On the contrary, if we look at the effect on the water−water correlations of the solute (cation plus anion), a more severe distortion of the hydrogen bond network may show up in the presence of the "structure maker" cation, due to the role of the anion in the same solution. Additionally at high solute concentration the counterion may affect also the ion hydration shell.[4]

Given the situation, ordering ions according to their ability as "structure breaker" or "structure maker" looks tricky, and the coincidence of such ordering with the ability of ions in salting in or out a protein, as described by the Hofmeister series,[13] is doomed to stay veiled. In this respect it has to be mentioned that while originally it was thought that the influence of an ion on macromolecular properties was at least partly caused by its influence on the water structure, recent experimental evidence[10] suggests that the structure of water may not be central to the Hofmeister effect. This needs instead to be understood in terms of direct interaction between the ions and macromolecules.[14,15]

In this paper, we present new neutron diffraction data from aqueous solutions of KSCN and compare the ion's solvation shells and water structure with those found in previous work on solutions of KCl[7,8] and KOH.[2,4] This will allow addressing the influence of the anion on the hydration shell of potassium, along with the issue of increasing influence of the anion on the water structure on going from $Cl^-$ to $OH^-$ and $SCN^-$. Moreover our determination of the solvation shell of the $SCN^-$ ion will be compared with those available in the literature, from neutron diffraction experiments on different salts solutions[15−17] and simulations.[18]

## II. Experiment and Data Reduction

The experiment has been performed at the SANDALS diffractometer,[19] installed at the ISIS pulsed neutron source (UK), on aqueous solutions of KSCN at ambient conditions and concentrations of 2.83, 1.31, and 0.66 mol, corresponding to one solute molecule per 17, 40, and 83 solvent molecules, respectively. All solutions have been prepared starting from commercially available products from Sigma-Aldrich, and their atomic densities, reported in Table 1, have been calculated from data available in the literature.[20] We have used standard Ti−Zr sample containers with 1 mm wall thickness and $t = 1$ mm sample thickness, which fit into the SANDALS sample changer. This allows a periodic exposure of the samples to the beam, while controlling the temperature through a water bath with external circulation; the sample temperature was set at 298.0 K and kept constant within ±0.1 K during the entire experiment. To apply the H/D contrast method in the neutron diffraction experiment, water hydrogens have been isotopically substituted and measurements have been performed on a fully deuterated solution, a fully protiated solution, and on an equimolar mixture of the two, making a total of 9 samples for the three

* To whom correspondence should be addressed. E-mail: riccim@fis.uniroma3.it.

† Present address: Material Physics Center, Joint Center CSIC-UPV/EHU, Paseo Manuel de Lardizabal 4, 200018 Donostia-San Sebastian, Spain.

10.1021/jp903462h CCC: $40.75 
Published on Web 07/01/2009

**TABLE 1: Lennard-Jones Parameters and Effective Atomic Charges Used to Start the EPSR Refinement of the Neutron Diffraction Data[a]**

| atom | $\varepsilon$ (kJ/mol) | $\sigma$ (Å) | $q$ (e) |
|---|---|---|---|
| O | 0.6500 | 3.1660 | −0.8476 |
| H | 0.0000 | 0.0000 | 0.4238 |
| K | 0.5144 | 2.9400 | 1.0000 |
| S | 1.5225 | 3.5200 | −0.5600 |
| C | 0.4250 | 3.3500 | 0.1400 |
| N | 0.3100 | 3.3100 | −0.5800 |

| sample | density (atoms/Å$^3$) | $L_{box}$ (Å) | $H_2O$ | $K^+$ | $SCN^-$ |
|---|---|---|---|---|---|
| 1:17 | 0.0916 | 30.96 | 840 | 50 | 50 |
| 1:40 | 0.0960 | 33.89 | 1206 | 30 | 30 |
| 1:83 | 0.0979 | 37.27 | 1662 | 20 | 20 |

[a] Sample concentration, expressed in molecules of solute per molecules of solvent, sample density and size of the EPSR simulation box, along with the number of water molecules, $K^+$, and $SCN^-$ ions in the box are reported in the bottom part of the table.

concentrations investigated. For each sample, data have been accumulated for about 12 h, with ISIS running on average at 180 $\mu$A; measurements have also been performed for the empty containers, empty instrument, and a standard vanadium slab (5.0 × 5.0 × 0.348 cm$^3$).

Data reduction has been performed by using the suite of programs (Gudrun)[21] available for SANDALS and widely described elsewhere.[22] This performs corrections for multiple scattering, absorption, and inelasticity effects, subtracts the sample container contribution, and normalizes the data to an absolute scale. Gudrun also performs a check of the sample density, $\rho$, and composition against the high $Q$ limit of the total measured differential scattering intensity, defined as

$$\lim_{Q\to\infty} I(Q) = \frac{\rho t \sum_{\alpha} c_\alpha \sigma_\alpha}{4\pi} \quad (1)$$

where $Q$ is the modulus of the exchanged wavevector and $c_\alpha$ and $\sigma_\alpha$ are the fraction and total scattering cross section[26] of atoms of type $\alpha$. The final output of the data reduction procedure is the neutron differential cross section (DCS)

$$F(Q) = \sum_{\alpha}\sum_{\beta>\alpha} c_\alpha c_\beta b_\alpha b_\beta (2 - \delta_{\alpha\beta})(S_{\alpha\beta}(Q) - 1) \quad (2)$$

where $b_\alpha$ is the neutron coherent scattering length[26] of the $\alpha$ species. $S_{\alpha\beta}$ is the partial structure factor (PSF), namely the Fourier transform of the RDF of the $\alpha,\beta$ pair:

$$S_{\alpha\beta}(Q) = 1 + 4\pi\rho \int_0^\infty r^2 (g_{\alpha\beta}(r) - 1)\frac{\sin(Qr)}{Qr}\,dr \quad (3)$$

Since hydrogen and deuterium have markedly different scattering lengths, the H/D substitution on the solute gives access to three independent DCS data sets at each ion concentration, characterized by a good contrast one to each other (see Figure 1). Each KSCN−water solution consists of $m = 6$ different atomic species (namely H/D, O, K, S, C, and N), consequently each DCS is the combination of $m(m + 1)/2 = 21$ distinct PSFs and complete exploitation of the microscopic structure of these solutions is subject to the inversion of a system of three equations with 21 unknowns (see eq 2), that are the individual

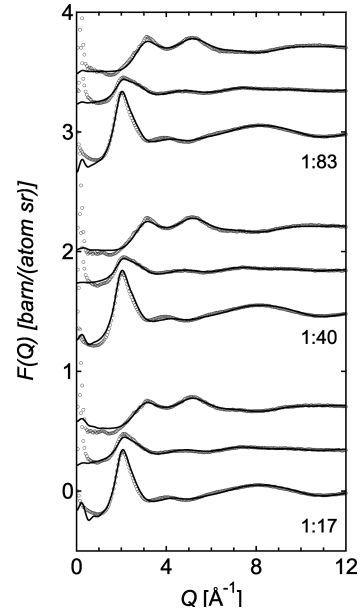


**Figure 1.** Comparison between the experimental data (circles) and the EPSR simulation (line) for the investigated KSCN−water solutions. Data have been shifted for clarity. At each concentration the DCS of the deuterated sample is at the bottom, that of the hydrogenated one on the top, and that of the mixture is in the middle.

PSFs. The solution of this inversion is not unique, and can only be performed with the support of a proper computer simulation model and based on complementary knowledge, such as for instance molecular geometry, presence of H-bonds between water molecules, etc.

In the present instance we have used the empirical potential structure refinement (EPSR)[23−25] code. Application of this code to studies of aqueous solutions are thoroughly described in refs 1−9 and 22. Briefly, this is a standard Monte Carlo simulation of the solution in question, which iteratively adjusts a perturbation to the starting reference potential until the simulated DCSs converge to a satisfactory fit of the measured data. This is usually achieved after hundreds of iterations, provided that the starting reference potential can mimic the relevant features of the system, such as the presence of a network of H-bonds in the present instance. Several different choices of this potential model may be reasonable, and many are available in the literature at least for water; nevertheless the experience over the years has demonstrated that the different choices do not dramatically affect the final result, when used within the EPSR code.[27,28] In particular the range of RDF compatible with the experimental data is usually rather narrow, although the degree of reliability of the individual RDF depends of course on its weight within the DCS functions. Specifically at low solute concentrations water−water RDF will have the higher weight, followed by solute-water ones, while solute−solute terms will give the lower contribution to the measured DCS. After convergence to a good fit, the EPSR simulation proceeds by accumulating molecular configurations compatible with the data.

The quality of the fits obtained for the present data is shown in Figure 1, where the DCS functions for all samples are reported along with the corresponding simulation. As reference potential we have used the SPC/E model[29] for water−water interactions and Lennard-Jones plus fractional charges for the solutes,[30] according to Table 1. The Lorentz−Berthelot rules have been applied for the interaction between different species. The simulation box dimensions and composition are reported in Table 1 for the individual solutions. The whole set of site−site

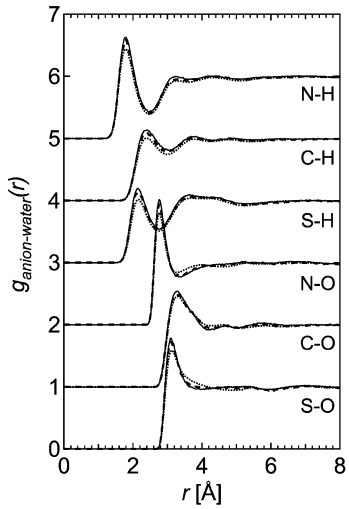


**Figure 2.** The anion hydration: site−site RDF for the individual $SCN^-$−water atomic pairs at all the investigated solutions. Solid, dashed, and dotted lines correspond to the 1:83, 1:40, and 1:17 concentrations, respectively. Data have been shifted for clarity.

RDF, along with other structural properties of interest, as for instance the distribution of bonding angles and the so-called spatial distribution functions (SDFs)[31] or the orientational correlation functions (OCFs)[31] around a given molecule or ion have been calculated after the accumulated molecular configurations. The SDFs and OCFs are evaluated through a spherical harmonic expansion of the relevant pair correlation function $g(\vec{r},\vec{\Omega}_1,\vec{\Omega}_2)$, $\vec{\Omega}_i$ being the Euler angles which define the orientation of the *i*th molecule. The SDF allows us to visualize in three dimensions the probability of finding a second molecule, whatever oriented, at a position $\vec{r}$ relative to a specified molecule at the origin. The OCF describes in turn the preferred orientation, $(\vec{\Omega}_2 - \vec{\Omega}_1)$, of a second molecule at a specified position relative to the central one.

## III. $SCN^-$ Hydration Shell

According to chemistry textbooks, the negative charge of $SCN^-$ is equally distributed on the S and N sites and consequently it is an ambidentate ligand, which can coordinate cations or water molecules at both ends. The effective potential model[30] available in the literature and used to start the EPSR simulation, indicates a small charge difference between the S and N site. Despite such small difference, our data suggest a clear asymmetry between the hydration shell of the two atomic sites, as shown in Figure 2 and 3. As a matter of fact the first H−S peak is at $r = 2.2$ Å and this distance looks far too long in order to achieve hydrogen bonding between hydrogen and sulfur atom. Moreover the SDF of water around the sulfur atom (see inset 3 of Figure 3) shows that the $C\hat{S}H$ angle between the anion axis and the S−H direction can vary in a broad range, suggesting that the orientational correlations between water and solute are weak.

Conversely, the first peak of $g_{NH}(r)$ is at 1.8 Å and the first peak of the $g_{NO}(r)$ is about 1 Å apart, suggesting that nitrogen atoms form a typical hydrogen bond with surrounding water molecules. The signature of a marked orientational correlation between water molecules first neighbors of the N atoms and the anion axis is indeed visible in the corresponding SDF (see inset 2 of Figure 3), where the isoprobability surface is distinctly sharper than that on the sulfur side. Integration over the first peak of $g_{NH}(r)$ gives a coordination number

$$n_{NH}(r) = 4\pi\rho_H \int_0^r r'^2 g_{NH}(r')\, dr' \quad (4)$$

ranging between 2.3 at the highest investigated solute concentration and 3.1 at the lowest. Importantly, preferential H-bonding at the N site has been previously reported in aqueous solutions of NaSCN. These earlier experimental works[15,17] were not supported by an atomistic simulation and consequently the individual site−site contributions to the total radial distribution functions were not separated; as a result, a single broad peak at about 2 Å was identified as due to H-bonding at the N site of the $SCN^-$ ion. The use of the EPSR code allows us to identify O−H and O−N contributions, as discussed above, and in particular we can identify the peak at 2.8 Å as due to the correlation between water oxygen and nitrogen, at odds with the claim made in ref 15 and with the consequent assumption on the existence of a *hydration bond*, different from a standard hydrogen bond, due to its primarily Coulombic nature.

Both $g_{CO}(r)$ and $g_{CH}(r)$ show a very broad first peak, at higher distances, $r \approx 3.4$ Å, compared to the other site−site RDFs, suggesting that the C site is the less accessible to water molecules. The SDF shows indeed (see inset 1 of Figure 3) that the neighboring water molecules lie within a belt, around the C site.

All RDFs and probability isosurfaces do not show a marked dependence on the solute concentration, suggesting that the egg-shaped hydration shell of the anion (see its 3D reconstruction in the inset 4 of Figure 3) is a stable feature of these solutions. However there is an asymmetry between the top and bottom of this hydration shell, because our data suggest that water molecules form a H-bond with the N site (top), and are instead weakly coordinated with the S site (bottom). This is confirmed by the OCF, reported in Figure 4: here the left-hand side

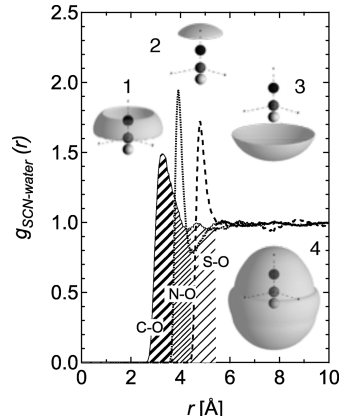


**Figure 3.** The SDFs for water around an $SCN^-$ ion oriented along the vertical axis *z* at concentration of 1 solute per 40 solvent molecules and contrast level of 0.2, are shown together with the $g_{CO}(r)$ function. The S atom is represented as a light gray sphere, the C atom as a middle gray sphere, the N atom as a dark gray sphere; the SDFs are labeled from 1 to 4. From left to right: The SDF 1 highlights the isoprobability surface for water molecules with an O−C distance between 2.7 Å and 3.7 Å, corresponding to the region of the $g_{CO}(r)$ function with the dark thick diagonals. The SDF 2 corresponds to water molecules at a distance from the C site between 3.7 Å and 4.4 Å, that is the region of the first C−O peak highlighted by thin diagonals: if we take into account the C−N intramolecular distance, these molecules are the first neighbors of the N site (see the shifted $g_{NO}(r)$ function, reported as a dashed line). The SDF 3 shows the isoprobability surface for water molecules at distance from the C site between 4.5 Å and 5.4 Å, that are first neighbors of the S site, as shown by the shifted $g_{SO}(r)$ function (long-dashed). The complete egg-shaped SDF (4) is shown at the bottom right-hand side.

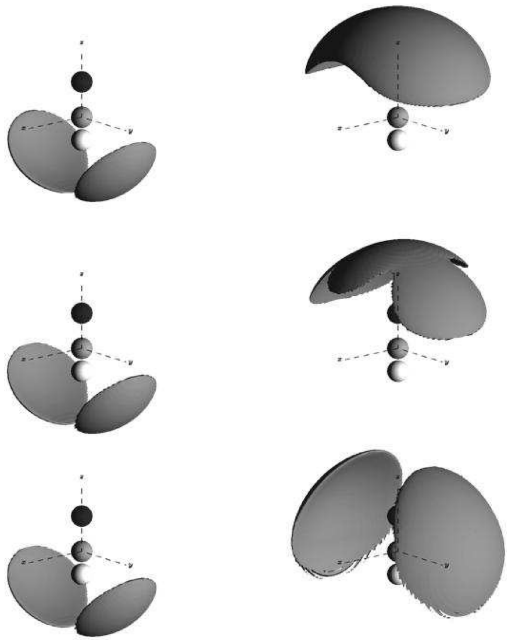

**Figure 4.** The OCFs for the first neighboring water molecules of the N and S site (corresponding to SDFs 2 and 3 of Figure 3), respectively, on the left and the right side; the solute concentration increases from the bottom to the top. The highlighted surfaces define the solid angle swept by the dipole moment of the water molecules neighboring the N (left) and S (right) sites and appear below or above the ion when the dipole moment points inward or outward. Accordingly the dipole moment of the molecules close to the N site points toward the ion and two quite well-defined preferred directions are identified, independently on the solute concentration: these are compatible with an almost linear H-bond. The direction of the dipole moment of molecules close to the S site is instead less well-defined and strongly dependent on the solute concentration.

describes the preferred orientations of the first neighboring molecules of the N site, the right-hand side describes those of the neighbors of the S site, and the concentration increases going from the bottom to the top. The highlighted surfaces define the direction where the dipole moment of the water molecules is likely pointing. Looking at this figure we notice immediately that the OCFs on the left do not change with concentration, contrarily to those on the right. More specifically water molecules likely H-bonded to the N site point their dipole moment toward the ion, as the OCFs lie below the horizontal plane: the angle between the OH−N direction and the dipole is compatible with an almost linear H bond, as also suggested by the sharpness of the first peak of the $g_{NH}(r)$ and of the relevant SDF (inset 2 from of Figure 3). The OCF relative to the orientation of water molecules' first neighbors of the S site (Figure 4) change shape and orientation with the solute concentration, indicating that the orientation of these molecules is determined by surrounding water rather than the ion; their isoprobability surfaces are also very broad, as those of the corresponding SDF (inset 3 of Figure 3), suggesting the presence of much weaker orientational correlations than those characteristic of an H-bond. The preferential hydration of the N site, compared to the S site, and the linearity of the hydrogen bonds made with surrounding water molecules lead therefore to the asymmetry shown in Figure 3, resulting in a water-depleted region around the $SCN^-$ ion along with the likely possibility of the S site to interact with other solutes more favorably than with water molecules.

The $SCN^-$ ion shares with $OH^-$ the asymmetric character of the hydration shell. Both ions have indeed H-bonded water molecules at one site and weakly correlated water molecules at the opposite site. They are strongly bonded to water at one extreme and in virtue of this can induce distortions to the water network, while the other extreme can easily loose its hydration water and be exposed to a solute. We notice however that the N−H bond-length, 1.8 Å, is larger than the H-bond length found in the case of $OH^-$, 1.4 Å,[4] although compatible with chemical literature.[32]

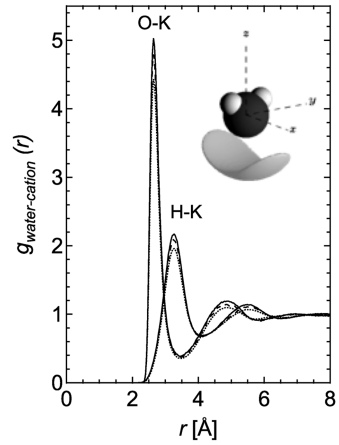


**Figure 5.** The cation hydration: $K^+$−water RDF for all the investigated solutions. Solid line refers to the concentration 1:83, dashed line to 1:40, and dotted line to 1:17. The SFD for the $K^+$ ions around a water molecule in the origin of the reference frame is reported at a contrast level of 0.20, as an inset.

## IV. $K^+$ Hydration Shell

The RDFs relative to the hydration shell of $K^+$ are reported in Figure 5 and show two well-defined neighboring shells, centered at the K−O distance $r \approx 2.6$ Å and $r \approx 4.8$ Å, respectively. The intensity of the first K−O peak decreases slightly with increasing salt concentration, and the corresponding coordination number drops from 5.9 to 4.6. These values compare well with those reported in the literature[33,34] for simulation of diluted $K^+$−$H_2O$ systems and neutron diffraction experiments on KCl aqueous solutions.[4,8,35] The lower number of neighbors at the highest investigated concentration may be ascribed to ion pairing phenomena although the number of water molecules is sufficient to completely hydrate both ions at all concentrations.

In the inset of Figure 5, we report the SDF for $K^+$ ions around a water molecule at 1:40 solute to solvent proportion, as a representative example, because no relevant changes of shape are evident as a function of concentration. This function shows that although the first peak of the $g_{OK}(r)$ function looks sharp and well-defined, the angle between the direction of the water dipole (or plane of the molecule) and the O−K direction is rather broad, as already found in previous experiments[4,8,35] when different counterions were present. Nevertheless a direct comparison of the O−K RDFs for three aqueous solutions at the same 1:83 concentration, but in the presence of different counterions, namely $Cl^-$, $OH^-$, and $SCN^-$, as reported in Figure 6, deserves a comment. It is indeed apparent that in the case of KCl and KSCN solutions the K hydration shells are almost coincident, while that of the KOH solution[35,36] has a larger minimum approach distance and first peak position; moreover, the first shell looks broader and less well-defined, while the second one is almost invisible. These characteristics were visible also at higher KOH concentrations[4] and were in agreement with the ab initio simulations of diluted $K^+$ solutions.[34] The differ-

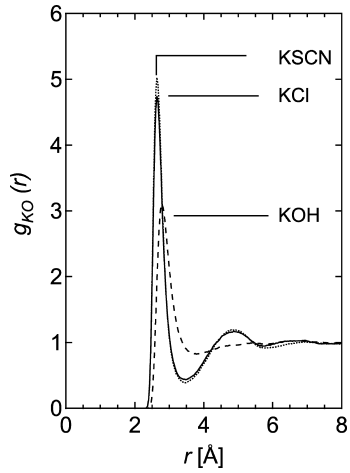


**Figure 6.** Comparison of $K^+$−water oxygen RDFs for different aqueous solutions at the same concentration (1:83). Data for the KCl,[8] KSCN, and KOH[35] solutions are reported as solid, dotted, and dashed lines, respectively.

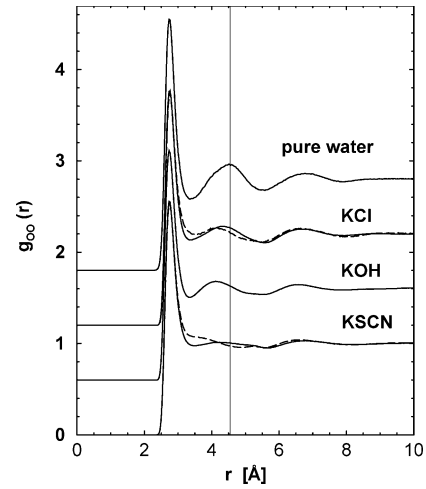


**Figure 7.** The oxygen−oxygen RDFs for water in the presence of potassium compounds are compared with that of pure water. For all solutions the solid line refers to the lowest (∼1:83) concentration and the dashed line to the highest (∼1:17) one. Data for KCl solutions have been redrawn from ref 7, those for KOH solutions at the lowest concentration are from ref 35. The solid vertical line marks the position of the second peak for pure water.[24]

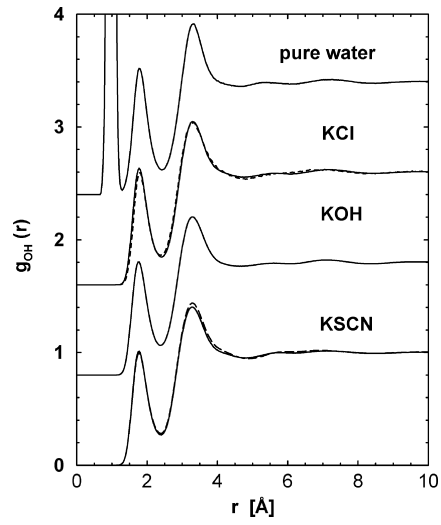


**Figure 8.** The oxygen−hydrogen RDFs for water in the presence of potassium compounds are compared with that of pure water. For all solutions the solid line refers to the lowest (∼1:83) concentration and the dashed line to the highest (∼1:17) one. Data for KCl solutions have been redrawn from ref 7, those for KOH solutions at the lowest concentration are from ref 35, those for pure water are from ref 24.

ences among the $K^+$ shells reported here may be due to the different balance between the $K^+$−water and anion−water interactions in the three solutions. As a matter of fact $OH^-$ forms shorter H-bonds than $SCN^-$ and $Cl^-$. The latter anion does indeed preferentially coordinate with water molecules along the O−H direction, but at an average distance from the water hydrogen of the order of ≥2 Å.[8] In other words, $OH^-$ is among the three anions the most efficient in coordinating its solvation shell, as suggested by the shortest H-bonds and due to its peculiar affinity with water, thus overwhelming the $K^+$ ion, which is left with a broader and "softer" hydration shell. This effect is not unlike what is found in computer simulations[37] when for a given ion size the solvation entropy increases due to a neat charge on the ion lower than ±1 e. On the other hand we cannot exclude that the differences shown in Figure 6 might be due to the lower fractional charge used in ref 4, 35 for the $K^+$ ion, a choice imposed by the request for similar charges on the oxygen and hydrogen sites of hydronium and SPC/E water.

## V. Water−Water Radial Distribution Functions

The RDFs for water in the presence of KSCN are reported for the highest and the lowest solute concentrations in Figures 7−9, along with those of pure water[24] and water in the presence of KCl[7] (at almost the same concentration as KSCN) and of KOH[35] at the 1:83 solute to solvent proportion. Changes of the $g_{OH}(r)$ and $g_{HH}(r)$ due to the presence of solutes are overall minor and weakly concentration dependent; nevertheless, we notice that the first two peaks of the $g_{HH}(r)$ function come closer one to the other and that the first peak of the $g_{OH}(r)$ function becomes less intense. The latter peak, centered at ∼1.8 Å, is the so-called H-bond peak, that is the signature of the presence of H-bonds between water molecules. The observation that its position does not change compared to pure water suggests that the strength of the H-bonding is not influenced by the presence of solutes, while the number of H-bonds per oxygen atom (evaluated according to the same definition given for the N−H bonds in eq 4) decreases from 1.68 to 1.47 in the case of KSCN solutions when the solute concentration increases.

The $g_{OO}(r)$ functions show clear and strong dependence on the solute concentration. In all solutions, when the solute concentration increases, the second peak moves to shorter distances and eventually becomes a shoulder of the first one. This peak is centered at ∼4.5 Å in pure water and is considered to be the signature of the presence of an extended H-bond network, since its distance from the first one is rationalized as due to an almost tetrahedral arrangement of neighboring molecules. It is known that its position moves to shorter distances when an external pressure is applied to pure water,[12,38] so that it has been proposed[2] that the effect of ions on the water structure could be described as an effective pressure. Within this framework, the effect of solvation of KSCN in water corresponds to the application of an effective pressure ranging from 150 and 600 MPa, with increasing concentration. That the intensity of this effective pressure and its range depends on the anion−cation pair has already been pointed out,[8] additionally here we want to stress that the solvation of KSCN has a qualitatively different effect on the tetrahedral order of water. As a matter of fact, by comparing the $g_{OO}(r)$ functions plotted in Figure 7 for the different solutions at the highest solute concentration, we notice that solvation of KSCN determines

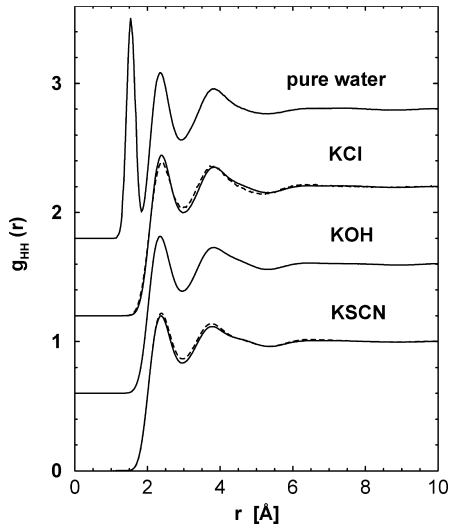


**Figure 9.** The hydrogen−hydrogen RDFs for water in the presence of potassium compounds are compared with that of pure water. For all solutions the solid line refers to the lowest (∼1:83) concentration and the dashed line to the highest (∼1:17) one. Data for KCl solutions have been redrawn from ref 7, those for KOH solutions at the lowest concentration are from ref 35, and those for pure water are from from ref 24.

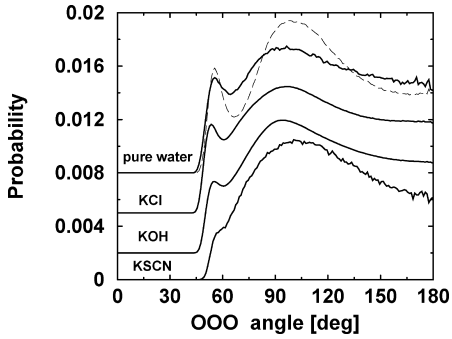


**Figure 10.** The distribution function of the OÔO angle formed by three neighboring water molecules at 1:83 solute concentration of KSCN, KOH, and KCl, compared with that of pure water[39] at two temperature values, namely, $T = 267$ K (dashed) and $T = 319$ K (solid), to show the possible variations around ambient conditions. Data have been shifted for clarity. Only minor differences are visible, with increasing ion concentration.

the maximum shift of the second peak; from the comparison of the RDFs at the lowest solute concentration KSCN looks instead as the less effective among the investigated solutes. Nevertheless even at the lowest concentration the overall shape of the second peak of the $g_{OO}(r)$ is clearly distorted in comparison with that of pure water as far as peak intensity and definition is concerned, contrarily to what found in the case of KCl and KOH solutions. The meaning of this difference can be better approached by analyzing the distribution functions of the OÔO angle formed by three neighboring water molecules (Figure 10). This distribution in pure water has a broad maximum centered at ∼104° and a sharper, although less intense, peak at ∼56°. The first one is the signature of the tetrahedral arrangement of first neighboring H-bonded water molecules, and the other is due to the presence of so-called interstitial molecules, that is, first neighbors not H-bonded molecules. In pure water when the temperature decreases both peaks become sharper as shown by the dashed and solid lines reported in Figure 10 for water at $T = 267$ K and $T = 319$ K, respectively. In the case of aqueous solutions, we notice that the peak ascribed to the interstitial molecules decreases on going from KCl to KOH and is almost

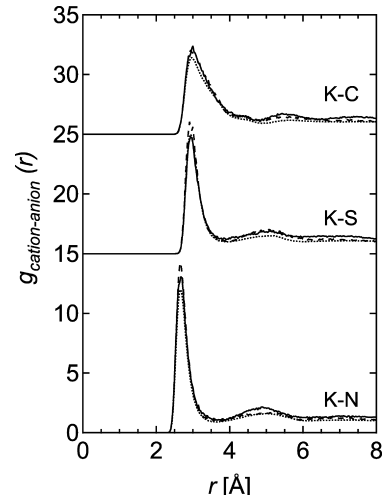


**Figure 11.** The $K^+-SCN^-$ RDF of all the investigated solutions: (solid line) 1:83 concentration, (dashed line) 1:40 concentration, and (dotted line) 1:17 concentration. K−S and K−C functions have been shifted for clarity.

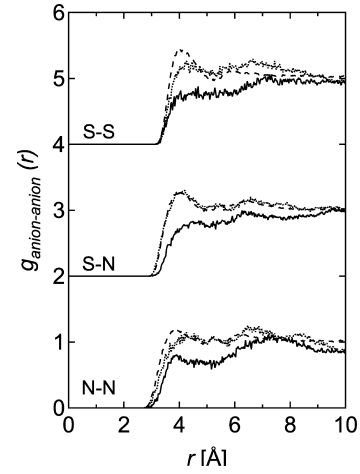


**Figure 12.** The S−S (shifted), S−N (shifted), and N−N RDF of all the investigated solutions: (solid line) 1:83 concentration, (dashed line) 1:40 concentration, and (dotted line) 1:17 concentration.

absent in KSCN. In the last case, we notice also a shift of the main peak to higher angles. The reduced number of interstitial molecules in KSCN solutions may be the microscopic counterpart of the lower density of water molecules in these samples, compared to other ionic solutions.[15]

## VI. Ion−Ion Correlations

Although bearing in mind that the ion−ion correlations are the less well determined in our analysis, still the anion−cation and anion−anion RDFs reported in Figures 11 and 12 deserve to be commented upon. The peak positions of the K-anion RDF are not concentration dependent, and suggest that ion pairing may occur at both ion sides, as expected for an ambidentate ligand. The minimum approach distance and average distance of the K−N pair are shorter that those of the K−S one, due to the smaller ionic radius of N. The broader peak of the K−C RDF is significant of the broadness of the ion contact angle. Integration over the first peak of $g_{KN}(r)$ and $g_{KS}(r)$ gives coordination numbers of ∼0.2 at the lowest concentration and ∼0.9 at the highest.

The S−S, S−N, and N−N RDFs (Figure 12) have a minimum approach distance of the order of 3 Å or higher and

the first maximum at ~4 Å. In particular at both anion sides both these distances are larger than their analogous distances for the O-anion and K-anion RDF, suggesting that anion−anion contacts are solvent or cation mediated.

## VII. Conclusions

The present study reports on a careful investigation of the microscopic structure of KSCN solutions. This has been accomplished by application of the EPSR code to analyze the neutron differential cross section, measured exploiting the H/D isotopic substitution at three different solute concentrations. In particular the ion's hydration shells, the water−water spatial correlations, and the issue of possible ion pairing have been addressed in detail. Indeed the EPSR routine builds a simulation box compatible with the experimental data and eventually allows the calculation of many structural functions of interest, which are not directly accessible by the experiment alone. As a matter of fact in an aqueous solution of KSCN, 21 distinct atomic pairs can be identified, thus no diffraction experiment can be exhaustive in determining each site−site radial distribution function and the angular correlations of interest. Combining experiments and simulations is therefore essential.

In the present paper we have compared the EPSR results with those of previous experiments performed, at about the same solute concentration, on solutions of KCl and KOH. This comparison has evidenced that although solvation of all these electrolytes has an effect on the microscopic structure of water similar to an external pressure, the solvation of KSCN is still peculiar: It gives the highest equivalent pressure at the highest solute concentration. More importantly, it determines an evident depression of the peak at 56° of the distribution function of the $\hat{OOO}$ angle formed by three first neighbors molecules. The latter observation suggests that the number of not H-bonded neighboring molecules is lower than in pure water.

As far as the hydration shell of the cation is concerned, the comparison suggests a possible influence of the anion, because the hydration shell in the presence of $OH^-$ is broader and centered at a larger distance compared to the case of KCl and KSCN solutions.

More interestingly our study has evidenced differences and similarities among the hydration shells of the anions. Among the three considered anions, $Cl^-$ fits the H-bond network of water better than the others and KCl solutions are the less effective in deforming the H-bond network of water. Both $OH^-$ and $SCN^-$ exhibit an asymmetric hydration shell, where neighboring water molecules form H-bonds at one side (with O and N, respectively) and are only weakly orientationally correlated at the opposite side (in the vicinity of H and S atoms, respectively). The number of H-bonds formed by the $OH^-$ is higher, their length is shorter, and the ion is globally more hydrophilic than $SCN^-$. This finding might explain the differences between the hydration shells of the cation as due to the balance of the interactions between different ionic species. Both $OH^-$ and $SCN^-$ weakly coordinate water molecules in the vicinity of H and S, respectively: this suggests that the anions might easily loose these hydration molecules, thus favoring their direct contact with other ions or solutes. This observation might be of particular relevance to explain the high protein crystallization efficiency of the $SCN^-$ ion.[40] One thiocyanate ion was found in crystals of egg-white lysozyme, with the ion bridging two symmetry-related protein molecules.[41] Importantly, the S atom of the ion has been found to form two direct intermolecular contacts with protein residues, and this is reasonably due to the low water affinity of this atomic site. Additionally we notice that $SCN^-$ is poorly hydrated in comparison to $OH^-$, as it forms approximately two H-bonds and has in total between 4 and 4.5 hydrogens in its first shell, while $OH^-$ forms four H-bonds and has 4 hydrogens and 1 water oxygen in its first neighbor shell. Poor hydration of $SCN^-$ was noticed also in ref 15, and this was suggested as one of the major reasons for the denaturant or salting-out effect of this ion.

On the basis of the above comparison between three anions we can conclude that the relative position of $Cl^-$, $OH^-$, and $SCN^-$ in the Hofmeister series seems to be correlated with their interaction with water, which becomes increasingly complex, eventually leading to an asymmetric hydration shell. In particlar $Cl^-$ can be solvated without dramatic distortions of the H-bond network, and its effect can be considered isotropic, as its solvation shell. $OH^-$ and $SCN^-$ induce more severe distortions of the H-bond network, although the origin of the distortions may be quite distinct, if we consider the different ion size, number and strength of the H-bonding. Nevertheless both these ions have an asymmetric neighbor shell and the peculiarity of being weakly coordinate at one-atomic-site with water molecules: this could contribute to increase the attraction of the larger poorly hydrated ions to nonpolar surface groups in a protein solution, as recently suggested by molecular dynamics simulations.[42]

**Acknowledgment.** The experiments on SANDALS have been performed within Agreement No. 06-20018 between CCLRC and CNR, concerning collaboration in scientific research at the spallation neutron source ISIS and with partial financial support of CNR. We would like to thank Mr. A. P. Russo of the Dipartimento di Fisica "E. Amaldi" (Università degli studi Roma Tre) for computer support. S. E. Pagnotta acknowledges a fellowship financed by CNISM, during the experiment.

## References and Notes

(1) Bruni, F.; Ricci, M. A.; Soper, A. K. *J. Chem. Phys.* **2001**, *114*, 8056.
(2) Botti, A.; Bruni, F.; Imberti, S.; Ricci, M. A.; Soper, A. K. *J. Chem. Phys.* **2004**, *120*, 10154.
(3) Botti, A.; Bruni, F.; Imberti, S.; Ricci, M. A.; Soper, A. K. *J. Chem. Phys.* **2004**, *121*, 7840.
(4) Imberti, S.; Botti, A.; Bruni, F.; Cappa, G.; Ricci, M. A.; Soper, A. K. *J. Chem. Phys.* **2005**, *122*, 194509.
(5) Botti, A.; Bruni, F.; Ricci, M. A.; Soper, A. K. *J. Chem. Phys.* **2006**, *125*, 014508.
(6) McLain, S. E.; Imberti, S.; Soper, A. K.; Botti, A.; Bruni, F.; Ricci, M. A. *Phys. Rev. B* **2006**, *74*, 094201.
(7) Mancinelli, R.; Botti, A.; Bruni, F.; Ricci, M. A.; Soper, A. K. *Phys. Chem. Chem. Phys.* **2007**, *9*, 2959.
(8) Mancinelli, R.; Botti, A.; Bruni, F.; Ricci, M. A.; Soper, A. K. *J. Phys. Chem. B* **2007**, *111*, 13570.
(9) Mancinelli, R.; Sodo, A.; Bruni, F.; Ricci, M. A.; Soper, A. K. *J. Phys. Chem. B* **2009**, *113*, 4075.
(10) Omta, A. W.; Kropman, M. F.; Bakker, H. J. *Science* **2003**, *301*, 347.
(11) Omta, A. W.; Kropman, M. F.; Woutersen, S.; Bakker, H. J. *J. Chem. Phys.* **2003**, *119*, 12457.
(12) Holzmann, J.; Ludwig, R.; Geiger, A.; Paschek, D. *Angew. Chem., Int. Ed.* **2007**, *46*, 8907.
(13) Kunz, W.; Lo Nostro, P.; Ninham, B. W. *Curr. Opin. Colloid Interface Sci.* **2004**, *9*, 1.
(14) Zhang, Y.; Cremer, P. S. *Curr. Opin. Chem. Biol.* **2006**, *10*, 658.
(15) Mason, P. E.; Neilson, G. W.; Dempsey, C. E.; Barnes, A. C.; Cruickshank, J. M. *Proc. Natl. Acad. Sci. U.S.A.* **2003**, *100*, 4557.
(16) Mason, P. E.; Dempsey, C. E.; Neilson, G. W.; Brady, J. W. *J. Phys. Chem. B* **2005**, *109*, 24185.
(17) Kameda, Y.; Takahashi, R.; Usuki, Y.; Uemura, O. *Bull. Chem. Soc. Jpn.* **1994**, *67*, 956.
(18) Sansone, R.; Ebner, C.; Probst, M. *J. Mol. Liq.* **2000**, *88*, 129.
(19) Soper A. K. In *Proceedings of the Conference on Advanced Neutron Sources 1988*; Institute of Physics and Physical Society: London, 1989.

Detailed information on the SANDALS diffractometer can also be found at the web site: www.isis.rl.ac.uk.

(20) Hoeiland, H.; Kvammen, O. J. *J. Chem. Eng. Data* **1983**, *28*, 179.

(21) See: www.isis.rl.ac.uk/disordered/dmgroup-home.htm. Accessed January 2009.

(22) Botti, A.; Bruni, F.; Mancinelli, R.; Lo Celso, F.; Triolo, R.; Ferrante, F.; Soper, A. K. *J. Chem. Phys.* **2008**, *128*, 164504.

(23) Soper, A. K. *Chem. Phys.* **1996**, *202*, 295.

(24) Soper, A. K. *Chem. Phys.* **2000**, *258*, 121.

(25) Soper, A. K. *Mol. Phys.* **2001**, *99*, 1503.

(26) Sears, V. F. *Neutron News* **1992**, *3*, 26.

(27) Bruni, F.; Ricci, M. A.; Soper, A. K. In *Conference Proceedings*; Societa' Italiana di Fisica: Bologna, Italia, 2000.

(28) Soper, A. K. *J. Phys.: Condens. Matter* **2007**, *19*, 415108.

(29) Berendsen, H. J. C.; Grigera, J. R.; Straatsma, T. P. *J. Phys. Chem.* **1987**, *91*, 6269.

(30) Vincze, A.; Jedlovszky, P.; Horvai, G. *Anal. Sci.* **2001**, *17*, i317.

(31) Svishchev, I. M.; Kusalik, P. G. *J. Chem. Phys.* **1993**, *99*, 3049.

(32) Jeffrey, G. A. In *An Introduction to Hydrogen Bonding*; Oxford University Press: New York. 1997.

(33) Grossfield, A. *J. Chem. Phys.* **2005**, *122*, 24506.

(34) Ramaniah, L. M.; Bernasconi, M.; Parrinello, M. *J. Chem. Phys.* **1999**, *111*, 1587.

(35) Corridoni, T. Ph.D. Thesis. Universita' degli Studi Roma Tre. Unpublished work.

(36) The $g_{OK}(r)$ function reported here for the 1:83 solute to solvent concentration has been obtained from the EPSR analysis of new neutron diffraction data, reported in ref 35 by using the same code and potential model used for the already published (ref 4) more concentrated solutions.

(37) Lynden-Bell, R. L.; Rasaiah, J. C. *J. Chem. Phys.* **1997**, *107*, 1981.

(38) Soper, A. K.; Ricci, M. A. *Phys. Rev. Lett.* **2000**, *84*, 2881.

(39) Ricci, M. A.; Bruni, F.; Giuliani, A. *Farday Discussion* **2009**, *141*, 347.

(40) Riès-Kautt, M.; Ducruix, A. *Methods Enzymol.* **1997**, *276*, 23.

(41) Howell, P. L. *Acta Cryst. D* **1995**, *51*, 654.

(42) Lund, M.; Jungwirth, P. *J. of Phys.: Condens. Matter* **2008**, *20*, 494218.

JP903462H